Sensor and Simulation Notes

Note 230

September 1977

Energy Confinement of a Bounded-Wave Simulator

F.C. Yang
K.S.H. Lee

Dikewood Corporation, Westwood Research Branch
Los Angeles, California

Abstract

The useful portion of the total transverse electromagnetic (TEM) power propagating in the conical as well as the cylindrical region of a bounded wave simulator is defined and calculated. It is found that the parallel plates offer better energy confinement than the conical plates.

Acknowledgement

Thanks go to Drs. C.E. Baum, J.P. Castillo, and K.C. Chen of the Air Force Weapons Laboratory for many enlightening discussions. We would also like to thank Dr. D. Giri for useful suggestions.

SECTION I
INTRODUCTION

In refs. 1 and 4, the impedance and field distribution of the transverse electromagnetic (TEM) mode on the conical section of the bounded wave simulator shown in figure 1 are given. Since this type of simulator is an open structure, the question may be asked as to how well the power from the generators is bounded by the simulator's structure. The present note deals exclusively with this question in the conical as well as the cylindrical section of the simulator by limiting the consideration to the TEM mode. A similar study has been made on the case where the conical section is considered to be two circular cones (ref. 5).

From the viewpoint of analytical tractability the best definition is first found in section II for the useful portion of the total power bounded by the simulator's structure. It turns out that this definition also leads to the ratio of the total charge per unit length on the bottom side of the top plate to the total charges per unit length on the two sides of the top plate. This is an important askew factor in other interaction problems where, for example, one may consider the effect a perfectly conducting ground may have on the charge distribution on the wing of an aircraft. This useful portion of the total power is numerically evaluated for two conical plates (section II) and for two parallel plates (section III). The results are graphically presented for various pertinent dimensions.

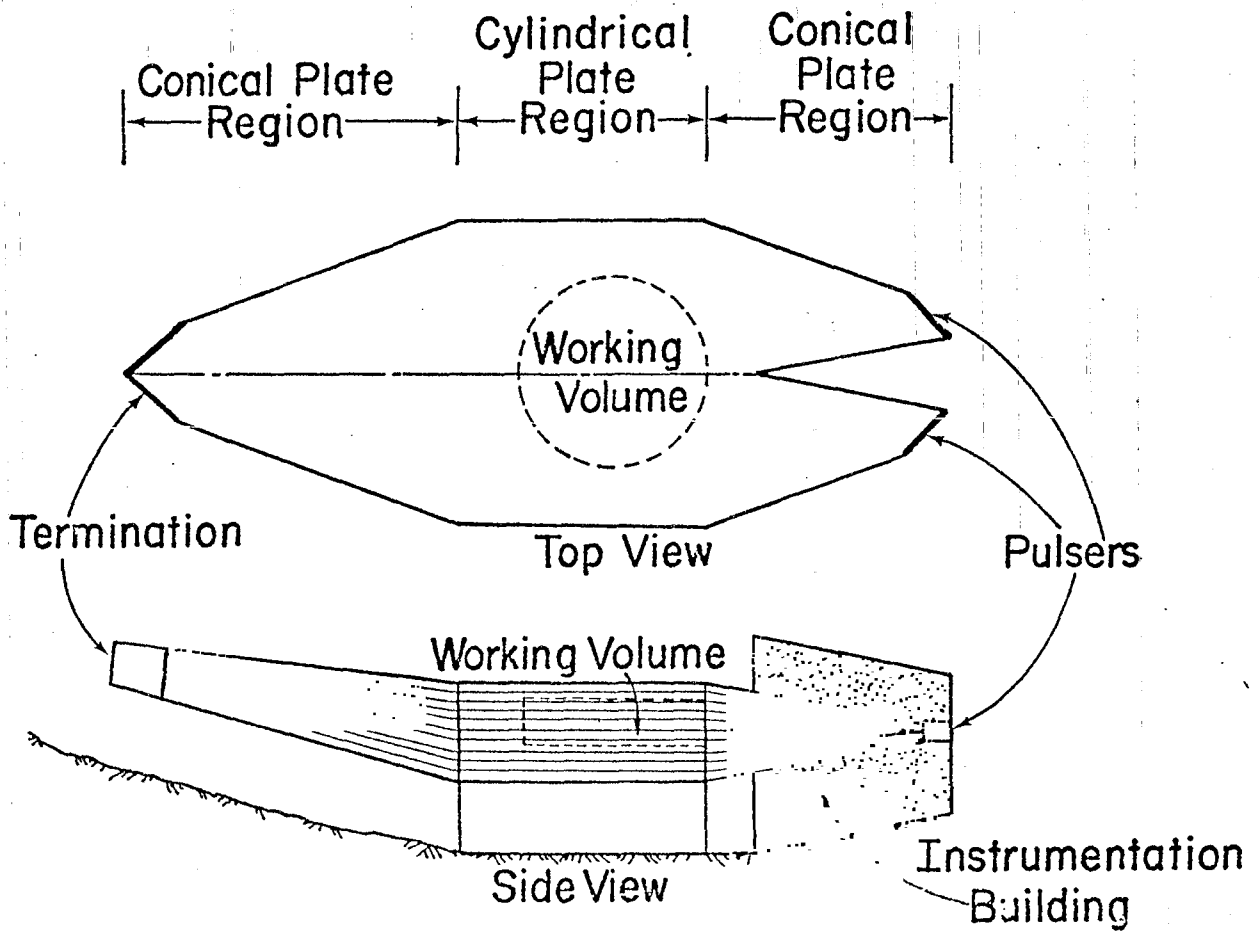

Figure 1. Top and side views of a bounded-wave simulator.

SECTION II
CONICAL REGION

In this section, the useful portion of the power launched onto a conical-plate transmission line is first defined and then calculated. Because the conical plates are open structures, the definition of useful power becomes somewhat ambiguous. Perhaps, the useful power can be defined as the total Poynting vector of the TEM mode crossing the area bounded by the two conducting plates and the electric-field lines emanating from the two edges of the upper plate and terminating at the two edges of the lower plate. In mathematical language, the fraction (f_e) of the total power that is useful in the above sense can be defined as

$$f_e = \frac{\int_{S_o} (\underline{E} \times \underline{H}) \cdot \hat{r}\, dS}{\int_{S_\infty} (\underline{E} \times \underline{H}) \cdot \hat{r}\, dS} \tag{1}$$

where S_∞ is the surface of the unit sphere and S_o is the part of S_∞ bounded by the two conical plates and the two electric field lines $\overline{CGC'}$ and $C_1G_1C_1'$ (see figure 2) connecting the plates.

There are two reasons for choosing S_o for the definition of useful power. First, the factor f_e as defined by equation (1) can be evaluated exactly to give a simple explicit result. Secondly, this factor, as will be shown shortly, is equal to the ratio of the total charge on the bottom side of the upper plate to the total charges on both sides of the upper plate. This ratio is quite useful in other interaction problems where the question is often asked about the effects the ground may have on the current and charge distributions on an otherwise isolated body in free space.

Of course, there are other ways of choosing S_o in equation (1). For instance, one may choose S_o to be the portion of S_∞ bounded by the two

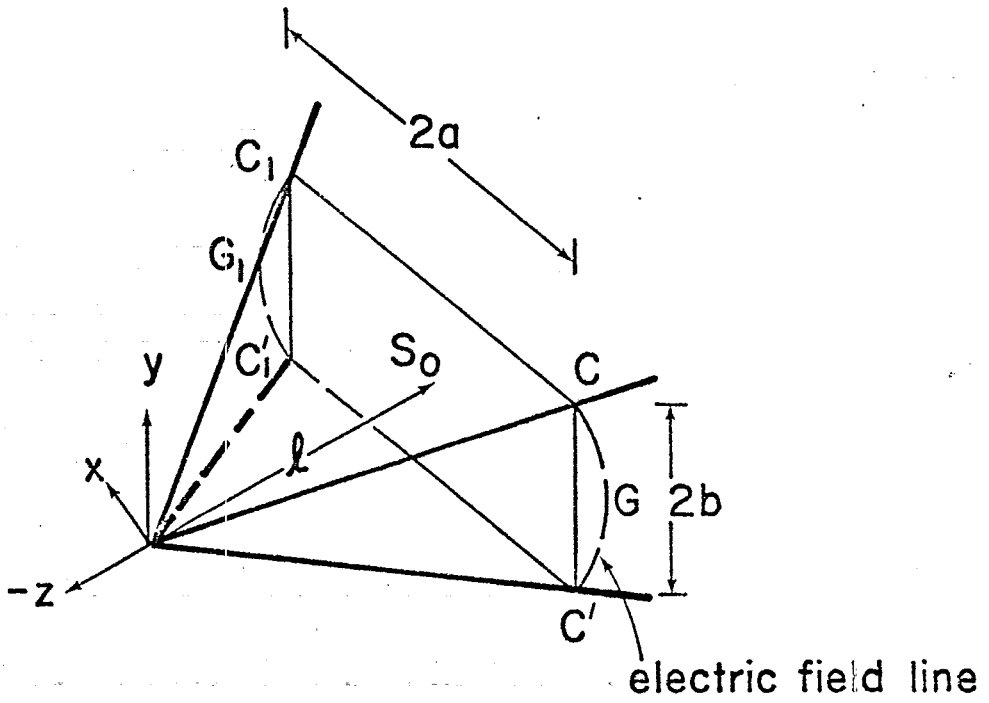

Figure 2. The surface S_o is bounded by the electric field lines CGC' and C_1GC_1' and the conical conducting plates.

plates and the straight lines CC' and C_1C_1', as shown in figure 2. Clearly, this definition of S_o will lead to a f_e-value smaller than that defined by the area $CGC'C_1'G_1C_1$. But this choice of S_o will make equation (1) very difficult to be evaluated and, hence, will not be pursued further in this report.

To show that expression (1) indeed reduces to the ratio of the two charges mentioned above one proceeds as follows

$$\int_{S_o} (\underline{E} \times \underline{H}) \cdot \hat{r}\, dS = \frac{1}{Z_o} \int_{S_o} \underline{E} \cdot \underline{E}\, dS$$

$$= -\frac{1}{Z_o} \int_{S_o} \nabla V \cdot \underline{E}\, dS$$

$$= -\frac{1}{Z_o} \int_{\ell_o} V \underline{E} \cdot \hat{r} \times d\underline{\ell} \qquad (\nabla \cdot \underline{E} = 0 \text{ , in } S_o)$$

$$= 2V_o c \int_{\ell_-} \sigma d\ell$$

$$= 2cV_o Q_- \qquad (2)$$

where Z_o is the free-space impedance; c is the free-space speed of light; σ is the charge density per unit length on the plates; ℓ_o is the line boundary of S_o; ℓ_- is part of ℓ_o immediately underneath the upper plate; $\pm V_o$ are the potentials of the upper and lower plate; and Q_- is the total charge per unit length on the bottom side of the upper plate. Similarly, if Q_+ denotes the total charge per unit length on the top side of the upper plate, one has

$$\int_{S_\infty} (\underline{E} \times \underline{H}) \cdot \hat{r}\, dS = 2cV_o (Q_+ + Q_-) \qquad (3)$$

Combining equations (2) and (3), one indeed obtains

$$f_e = \frac{Q_-}{Q_+ + Q_-} \tag{4}$$

which also means that f_e represents the fraction of the total energy bounded by the area S_o. Thus, f_e is a measure of the energy confinement of a bounded-wave simulator.

In ref. 1, the conical-plate problem is treated by using the stereographic and conformal transformations. The successive steps of the transformations are summarized in figure 3. These transformations map the first quadrant of S_∞ (i.e., the area with $x \geq 0$, $y \geq 0$) onto the rectangle ABDE in the W-plane. Concurrently, the first quadrant of S_o is mapped onto a sub rectangle CDEG. Since the fields are uniformly distributed within these rectangles, an inspection of figure 3 immediately gives

$$f_e = \frac{CD}{BD} = \frac{1}{2} + \frac{1}{2K(m)} F(\sin^{-1}[(1 - A_1)/\sqrt{n}]\,|\,m) \tag{5}$$

where n, m, A_1 are given in ref. 1. Expression (5) is plotted in figures 4 and 5 for various ℓ/b and b/a values. As expected, the factor f_e increases as b/a or ℓ/b is increased.

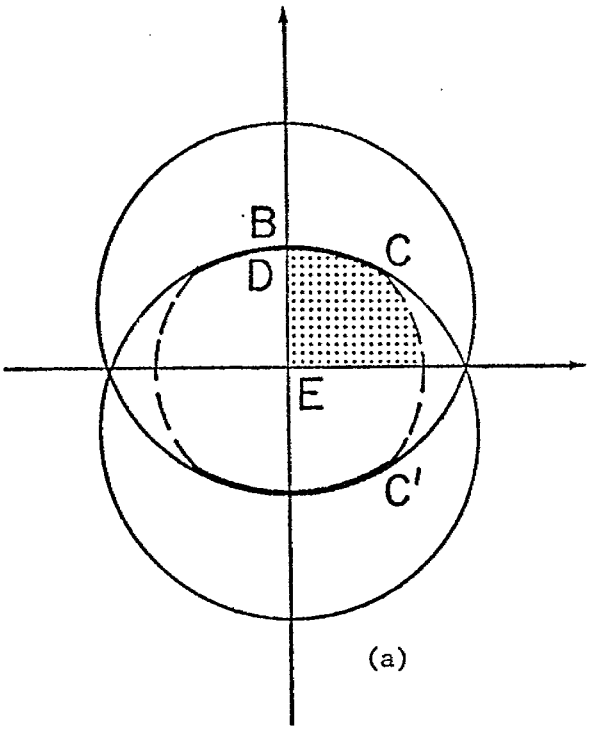

(a)

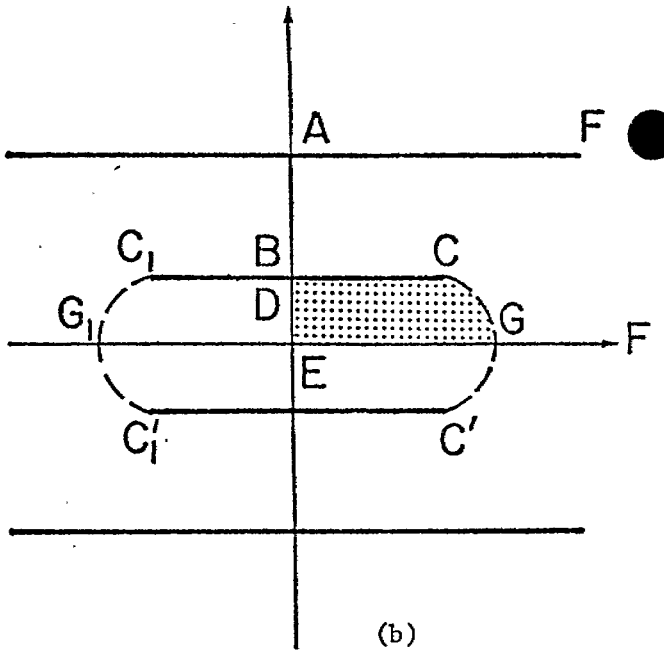

(b)

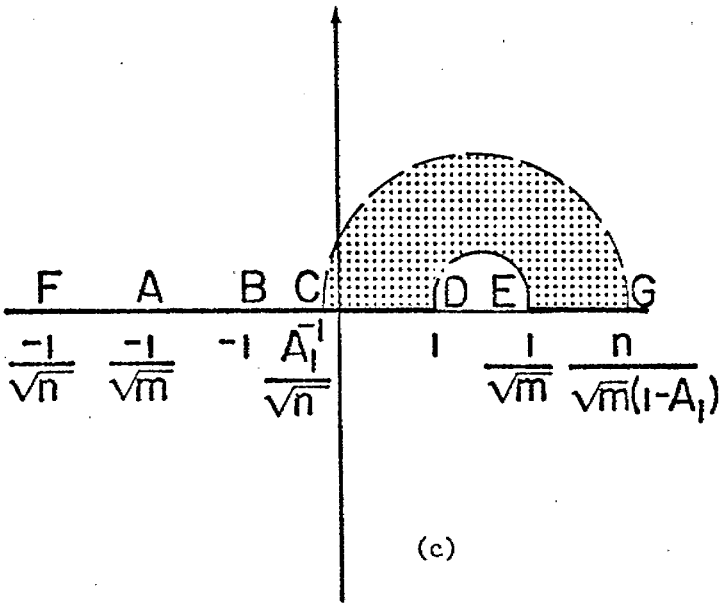

(c)

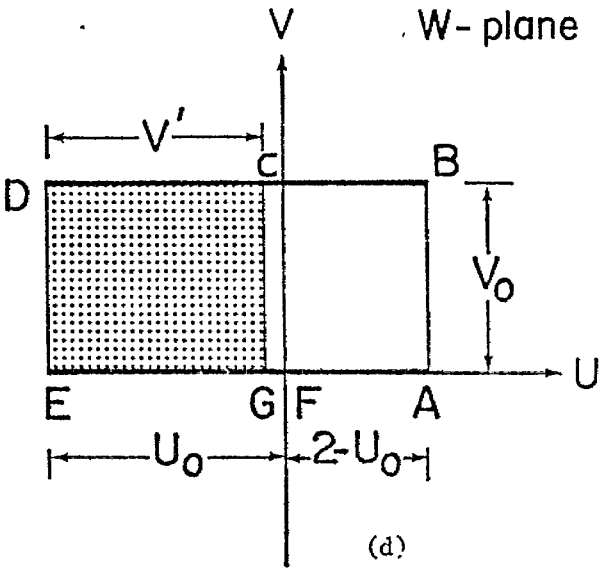

(d)

$$U_o = 1 + F(\sin^{-1}\sqrt{n/m}\,|\,m)/K(m)$$

$$V_o = K'(m)/K(m)$$

$$V' = 1 + F(\sin^{-1}[(1 - A_1)/\sqrt{n}]\,|\,m)/K(m)$$

Figure 3. Successive conformal transformations used for two conical plates.

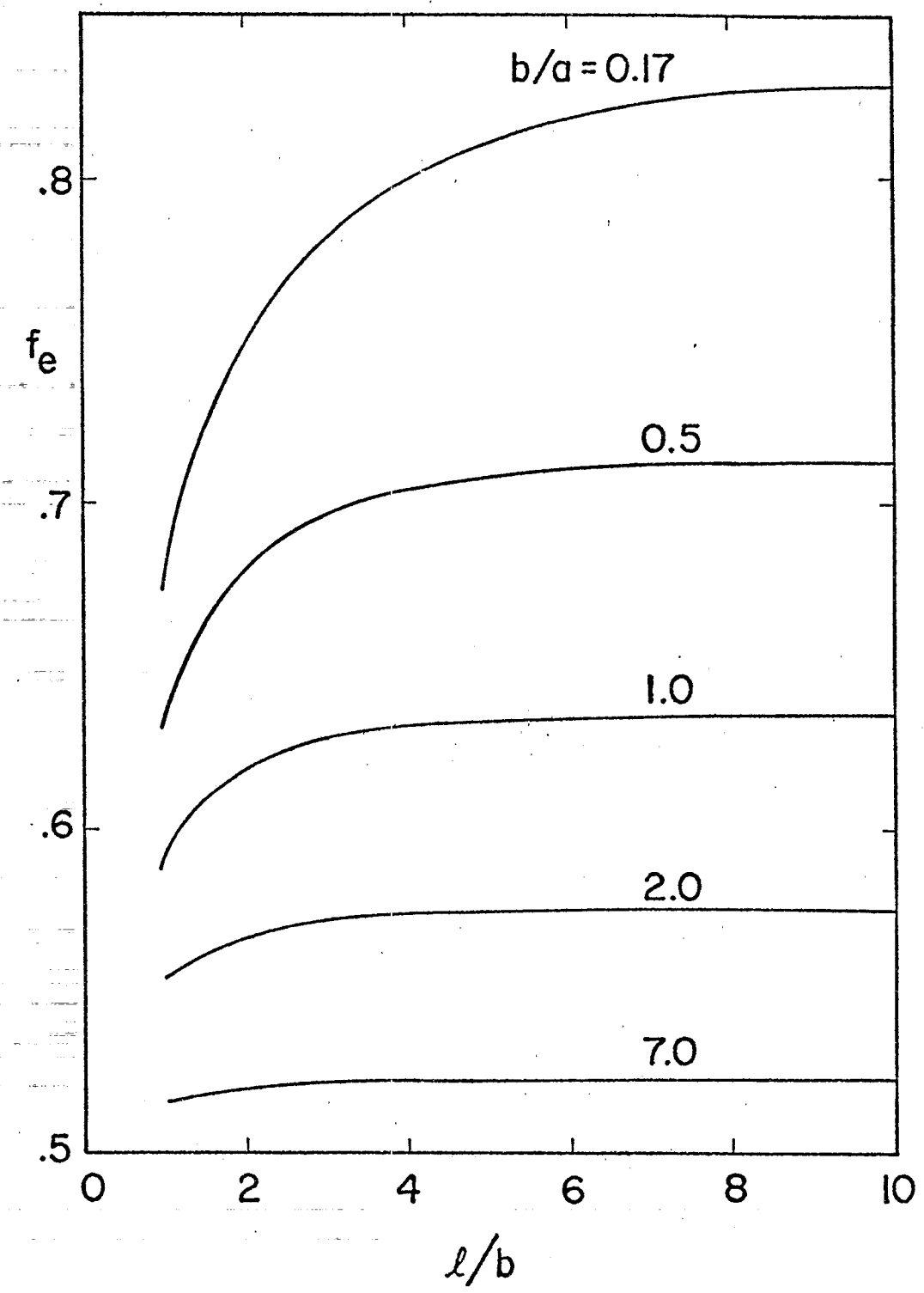

Figure 4. Energy confinement factor f_e of a two-conical-plate simulator versus ℓ/b .

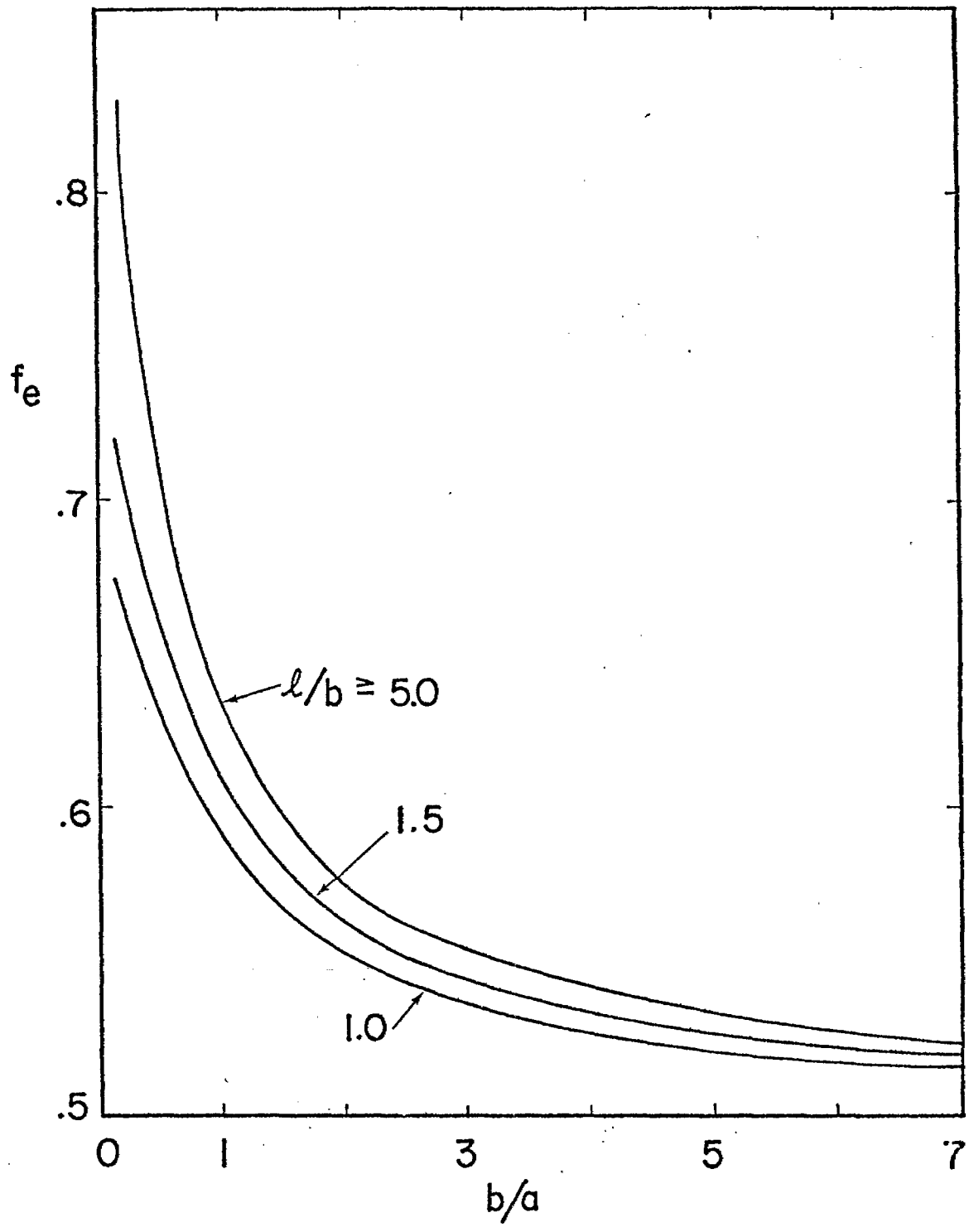

Figure 5. Energy confinement factor f_e of a two-conical-plate simulator versus b/a .

SECTION III

CYLINDRICAL REGION

The analysis of the preceding section can be applied directly to a two-parallel plate simulator shown in figure 6. Now expression (1) takes the form

$$f_e = \frac{\int_{S_o} (\underline{E} \times \underline{H}) \cdot \hat{z}\, dS}{\int_0^\infty \int_0^\infty (\underline{E} \times \underline{H}) \cdot \hat{z}\, dx dy} \tag{6}$$

where S_o is the dotted area shown in figure 6. Clearly, the symmetry property of the problem has been used in expression (6).

In refs. 2 and 3, the parallel-plate problem is solved by the technique of conformal mapping. The first quadrant of the complex z-plane is mapped onto the rectangle ABCE in the W-plane within which the field is uniformly distributed (see figure 7). The dotted area S_o is also mapped onto the dotted sub-rectangle HBCD . From figure 7, one immediately writes down

$$f_e = \frac{CD}{CE} = \frac{1}{K(m)} F(\sin^{-1}\sqrt{(E - m'K)/(mE)}\,|\,m) \tag{7}$$

where m is given in refs. 2 and 3. It should be pointed out that the parameter m in equation (7) is different from the parameter m used for the two conical plates. Equation (7) is numerically evaluated and the results are plotted in figure 8 in which the energy confinement factor f_e for two conical plates is also given for comparison. In figures 9 and 10 the ratio of the conical to the parallel-plate energy confinement factor is plotted versus b/a and ℓ/b, respectively. It can be seen from the figure that for the same b/a value the parallel-plate geometry gives a better energy confinement, as expected on physical grounds.

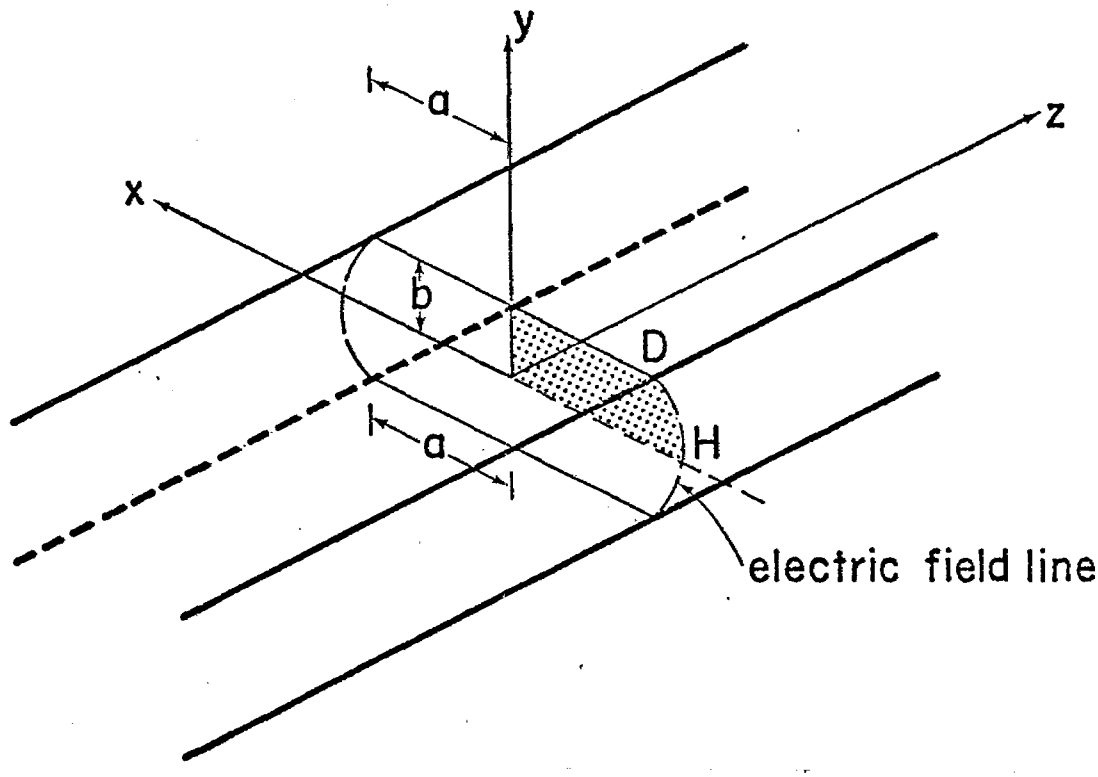

Figure 6. The dotted area is one-fourth the area for defining the energy confinement factor for a two-parallel-plate simulator.

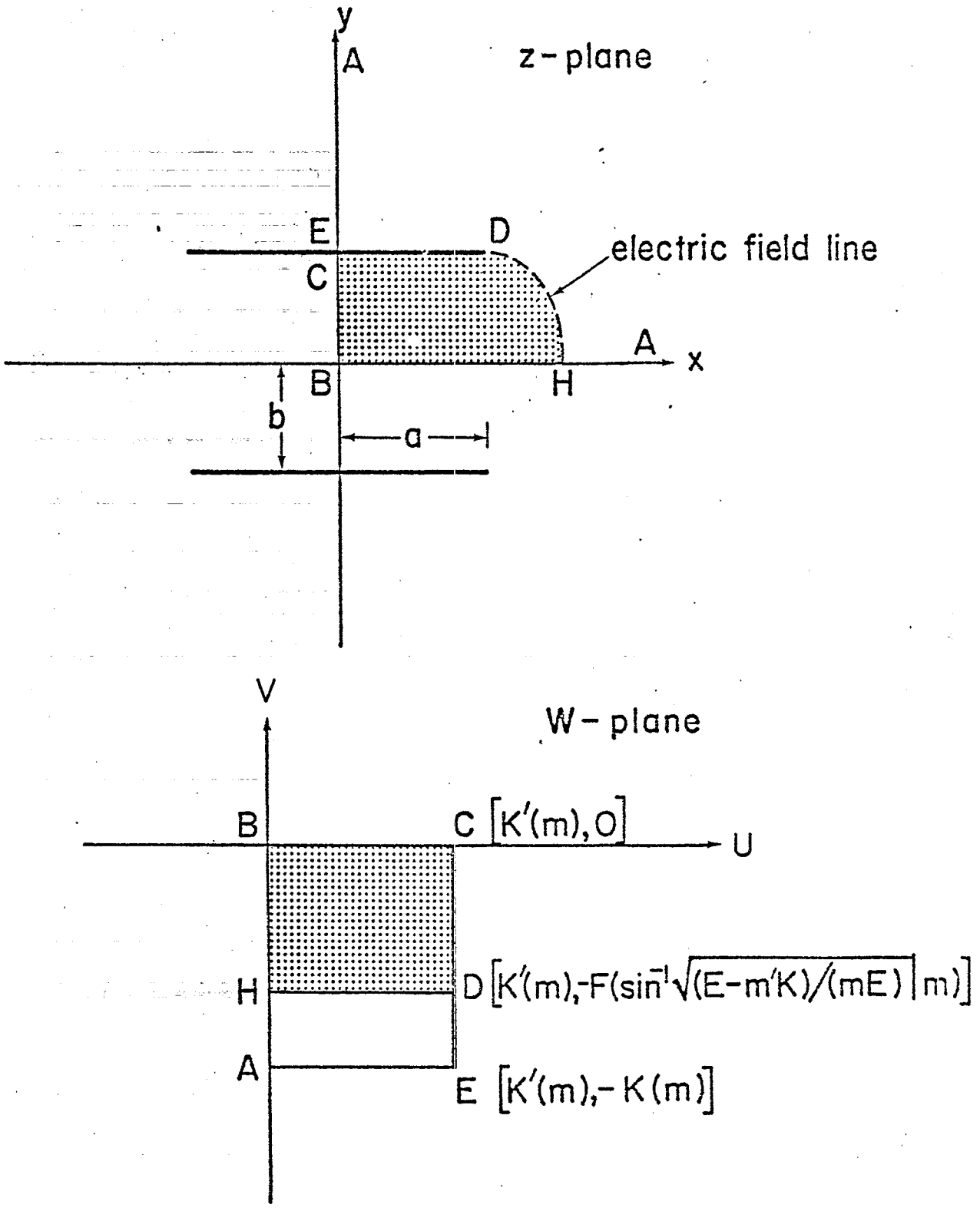

Figure 7. Conformal transformation of the complex coordinate (z) plane onto the complex potential (W) plane. (Note that the dotted area of the top diagram is conformally mapped onto the dotted area of the bottom diagram.)

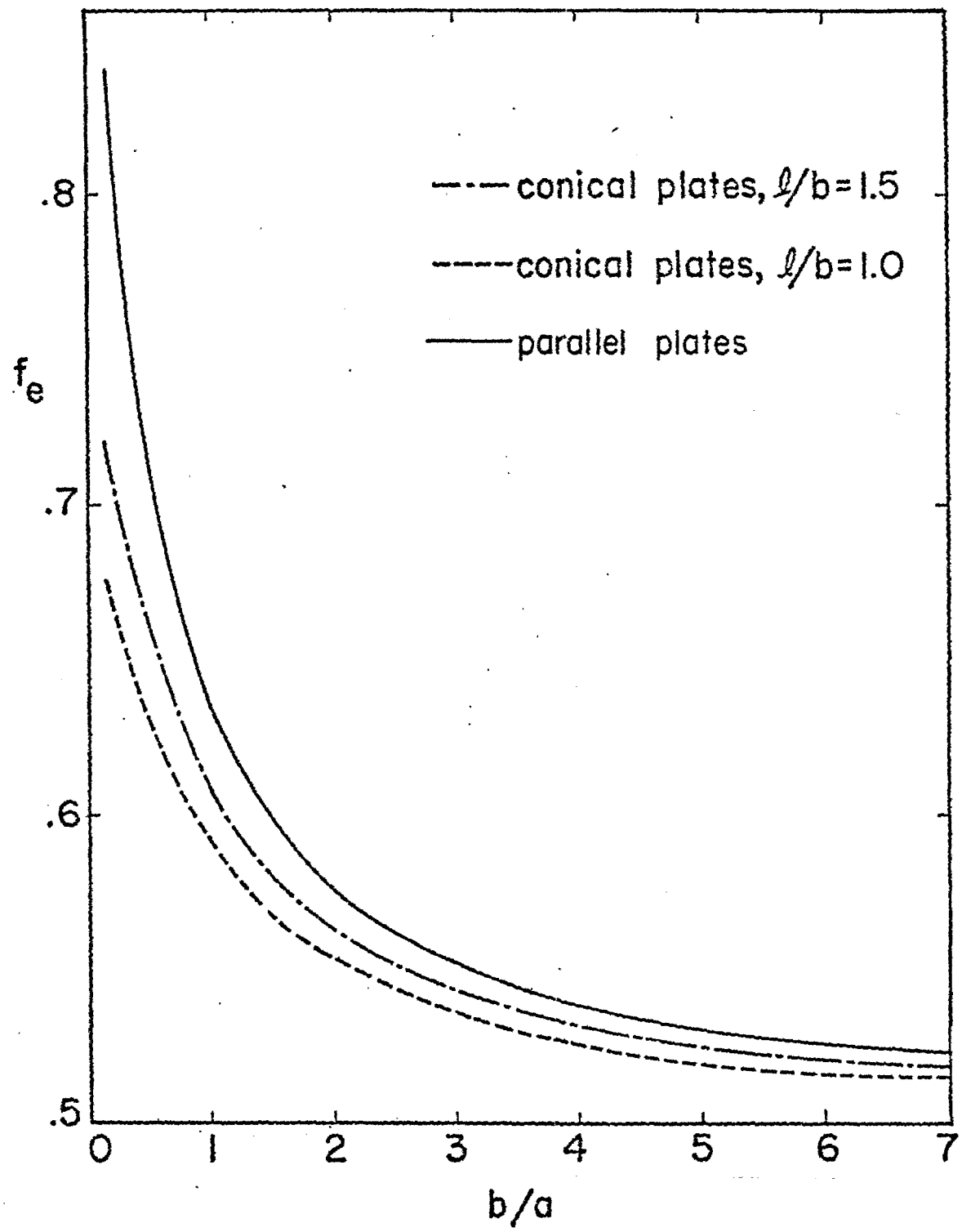

Figure 8. Energy confinement factor f_e of a two-parallel-plate simulator.

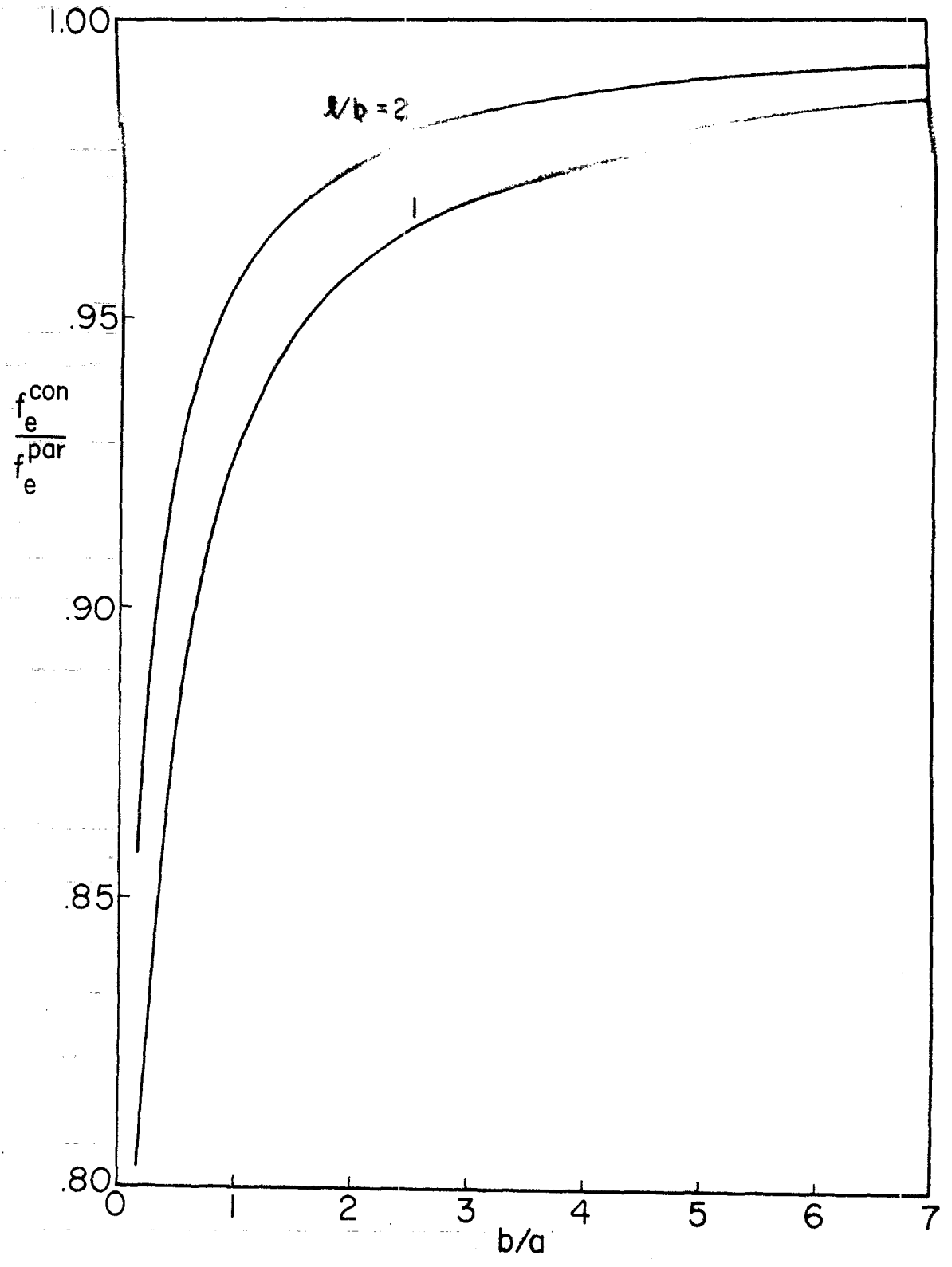

Figure 9. Ratio of the conical to the parallel-plate energy confinement factor versus b/a .

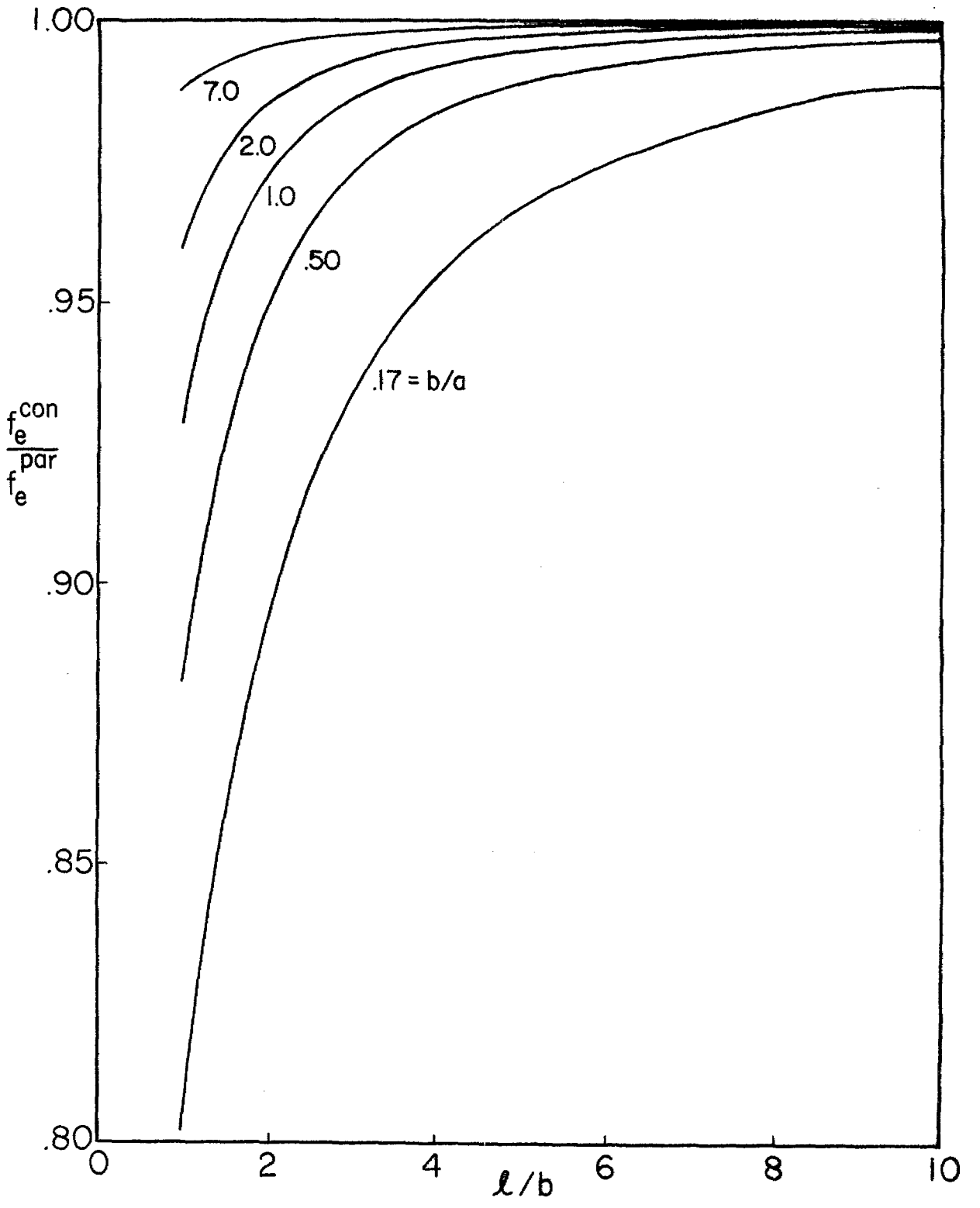

Figure 10. Ratio of the conical to the parallel-plate energy confinement factor versus ℓ/b .

REFERENCES

[1] F.C. Yang, K.S.H. Lee, "Impedance of a Two-Conical-Plate Transmission Line," Sensor and Simulation Note 221, November 1976.

[2] C.E. Baum, "Impedances and Field Distributions for Parallel Plate Transmission Line Simulators," Sensor and Simulation Note 21, June 1966.

[3] C.E. Baum, D.V. Giri, R.D. Gonzalez, "Electromagnetic Field Distribution of the TEM Mode in a Symmetrical Two-Parallel-Plate Transmission Line," Sensor and Simulation Note 219, April 1976.

[4] F.C. Yang, L. Marin, "Field Distributions on a Two-Conical-Plate and a Curved-Cylindrical-Plate Transmission Line," Sensor and Simulation Note 229, September 1977.

[5] R.W. Latham, M.I. Sancer, A.D. Varvatsis, "Matching a Particular Pulser to a Parallel-Plate Simulator," Circuit and Electromagnetic System Design Note 18, November 1974.